FULL PAPER

ADVANCED FUNCTIONAL MATERIALS

DOI: 10.1002/adfm.200700419

Autonomic Healing of Epoxy Vinyl Esters via Ring Opening Metathesis Polymerization**

By *Gerald O.Wilson*, *Jeffrey S. Moore*,* *Scott R. White*, *Nancy R. Sottos*, and *H. Magnus Andersson*

A materials system for autonomic healing of epoxy vinyl esters is demonstrated. The system is comprised of wax microspheres containing Grubbs' catalyst and microcapsules containing *exo*-dicyclopentadiene (DCPD) embedded together in an epoxy vinyl ester matrix. Healing is triggered when damage in the form of a crack ruptures the microcapsules, causing DCPD to be released into the crack plane where it comes in contact and mixes with the catalyst microspheres initiating ring opening metathesis polymerization (ROMP). The chemical compatibility of the catalyst with the matrix is investigated and wax protection of the catalyst via microspheres of a sufficient size (34–98 μm) is shown to provide a suitable barrier for protecting the catalyst from free radicals generated *in situ* during the curing of the epoxy vinyl ester resin. Wax protection of the catalyst also allows uninhibited curing of the matrix to proceed at room temperature. Concentration of self-healing components is varied with a view towards optimization of the recovery of virgin mechanical properties. Efficient self-healing is observed with microspheres that are smaller than those used in previous polymer matrices. Significant recovery of virgin mechanical properties is observed within 2.5 min of healing time at room temperature and the mechanical properties of healed samples after 24 h of healing time match those of existing ROMP-based self-healing systems.

1. Introduction

Self-healing polymers are a class of smart materials capable of autonomic repair of damage without the need for detection or repair by manual intervention.[1–10] Our group has previously reported ring opening metathesis polymerization[11] (ROMP)-based self-healing materials in which the Grubbs' catalyst is encapsulated in paraffin wax microspheres.[5] These wax microspheres serve the dual purpose of protecting the catalyst from deactivation by the diethylenetriamine (DETA) used to cure the epoxy matrix, and improving the dispersion of catalyst throughout the epoxy matrix. This protection and improved dispersion of catalyst resulted in a 90 % decrease in the catalyst concentration required to achieve similar levels of healing efficiency as in systems in which the catalyst phase was unprotected. Protecting the catalyst from aggressive curing agents by encapsulation in wax microspheres increases the versatility of the ROMP-based healing chemistry and enables its use in other matrices with similarly aggressive curing agents.

Epoxy vinyl ester resins (Fig. 1a) are used extensively in commercial products. As the matrix phase in reinforced composites, epoxy vinyl esters are used to produce large structural parts that are manufactured and cured at room temperature in an economical fashion without employing an autoclave. The curing chemistry of epoxy vinyl esters is based on the free radical-initiated polymerization of vinyl groups by a tertiary amine-peroxide initiation system. Free radicals produced by this initiation system are expected to have harmful effects on the Grubbs' catalyst used in ROMP-based self-healing. In this paper, we report on the chemical incompatibility of ROMP self-healing chemistry (Fig. 1b) with the epoxy vinyl ester curing chemistry, and demonstrate a viable healing system following wax protection of the catalyst. The size and concentration of wax microspheres in the epoxy vinyl ester matrix and the required amount of healing agent delivered to the crack plane for efficient self healing are optimized. While crack repair in epoxy vinyl ester has previously been reported,[12] the healing chemistry employed (PDMS-based) was not designed for struc-

[*] Prof. J. S. Moore
Department of Chemistry
University of Illinois at Urbana-Champaign
600 S. Mathews Ave., Urbana, IL 61801 (USA)
E-mail: jsmoore@uiuc.edu
Prof. J. S. Moore, G. O. Wilson, Prof. S. R. White, Prof. N. R. Sottos, H. M. Andersson
Beckman Institute
University of Illinois at Urbana-Champaign
405 N. Mathews Ave., Urbana, IL 61801 (USA)
G. O. Wilson, Prof. N. R. Sottos
Department of Materials Science and Engineering
University of Illinois at Urbana-Champaign
1304 W. Green St., Urbana, IL 61801 (USA)
Prof. S. R. White
Department of Aerospace Engineering
University of Illinois at Urbana-Champaign
104 S. Wright St., Urbana, IL 61801 (USA)

[**] This work has been sponsored by the UIUC Grainger Emerging Technology Program, Northrop Grumman Ship Systems and the Air Force Office of Scientific Research Sponsored Multidisciplinary University Research Initiative (MURI). The authors gratefully acknowledge helpful discussions with Dr. J. Rule, Dr. H. Weissman, and Dr. S. Cho. Electron microscopy was performed in the Imaging Technology Group, Beckman Institute at the University of Illinois at Urbana-Champaign with the assistance of S. Robinson.

ADVANCED FUNCTIONAL MATERIALS

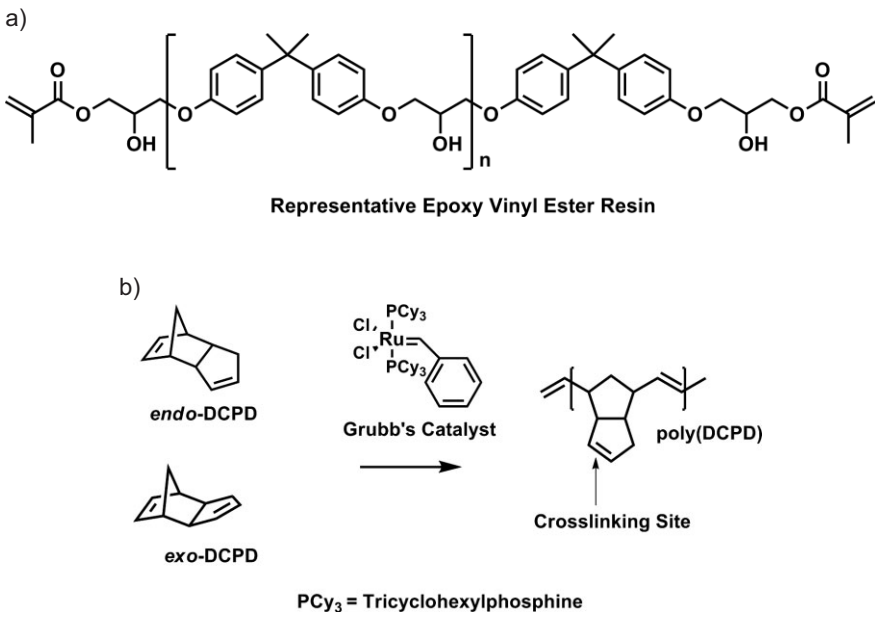

Figure 1. Self-healing chemistry in epoxy vinyl esters. a) A representative epoxy vinyl ester resin. Most resins contain reactive diluents, such as styrene in the case of the Derakane 510A-40 resin used in the experiments reported here. b) Ring opening metathesis polymerization (ROMP) of DCPD.

tural polymers and composites where recovery of mechanical properties is of paramount importance.

2. Results and Discussion

A successful self-healing chemistry requires that the healing agents remain inert during the matrix manufacturing process and during the lifetime of the self-healing material. Preventing chemical reactions between the healing agents and the matrix polymer resin during curing is essential both for preserving self-healing functionality and to avoid deleterious effects to the matrix. For self-healing epoxy vinyl esters, the chemical compatibility of the resin curing agents, benzoyl peroxide (BPO) and dimethylaniline (DMA), with Grubbs' first generation catalyst was investigated.

Catalyst stability was monitored by solution ^{1}H NMR spectroscopy. The intensity of the resonance associated with the carbene proton (δ = 20.62 ppm) was monitored in the presence of BPO (1 wt %) or DMA (0.1 wt %) or both. These specific curing agent concentrations were chosen to simulate the standard curing conditions of the epoxy vinyl ester matrix used in this study. While DMA alone had no effect on the catalyst, the intensity of the carbene proton peak was observed to diminish at a significant rate in the presence of BPO and at an even faster rate in the presence of both BPO and DMA (Fig. 2). The reaction between the free radicals generated *in situ* and Grubbs' catalyst also disrupts the curing of the epoxy vinyl ester resin. To illustrate this, resin samples were monitored by differential scanning calorimetry (DSC) under isothermal (25 °C) conditions both in the presence (2.5 wt %) and absence of catalyst for 2 h. The presence of Grubbs' catalyst drastically slowed the curing process with a degree of cure of only 4 % observed after 2 h (Fig. 3; 5). In contrast, samples without Grubbs' catalyst cured to greater than 80 % in the same time under otherwise identical conditions (Fig. 3; 1). Moreover, samples containing catalyst still remained ductile after 24 h suggesting that an acceptable degree of cure cannot be attained at room temperature within a reasonable period of curing time.

Protection from harmful curing agents in analogous self-healing materials has been achieved by embedding Grubbs' catalyst in paraffin wax microspheres.[5] Up to 69 % of the catalyst activity was preserved in 90 μm diameter wax microspheres containing 5 wt % Grubbs' first generation catalyst in the presence of DETA, which otherwise deactivated the catalyst completely. A similar study was carried out here to test the stability of wax protected Grubbs' catalyst upon exposure to BPO and DMA. Wax microspheres containing 10 wt % Grubbs' first generation catalyst were prepared using slight variations of established procedures[5] to yield three size ranges with average diameters of (98 ± 69) μm, (53 ± 31) μm, and (34 ± 13) μm (Fig. 4).

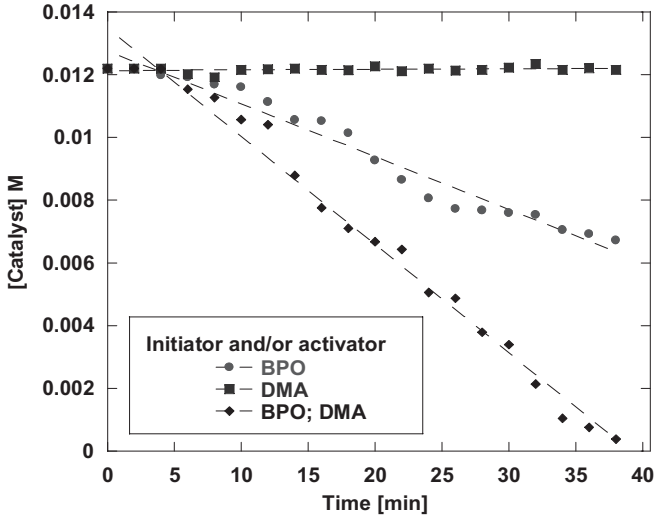

Figure 2. Effect of curing agents BPO and DMA on Grubbs' catalyst at 25 °C. The intensity of the carbene proton (δ = 20.62 ppm) is monitored (in benzene-d_6, by ^{1}H NMR spectroscopy) as a function of time using mesitylene as an internal standard. The concentrations of BPO (1 wt %, 0.041 M) and DMA (0.1 wt %, 0.0083 M) mimic actual curing conditions.

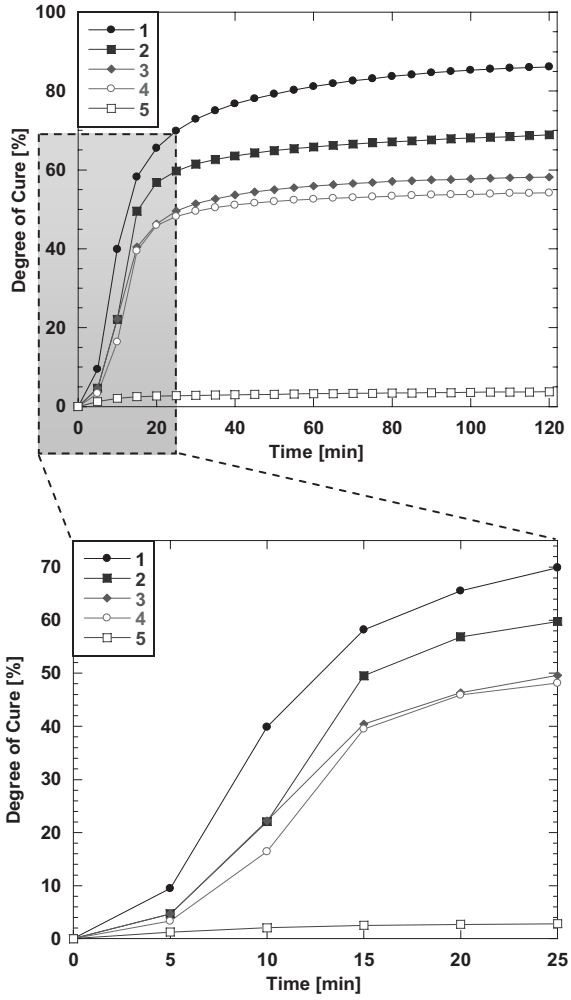

Figure 3. Effect of catalyst on the cure kinetics of the epoxy vinyl ester matrix as determined by isothermal Differential Scanning Calorimetry (DSC) experiments. A control experiment (1) contains no catalyst in the resin. The catalyst is incorporated into the matrix in its protected form in wax microspheres (10 wt % added to the resin) of diameters 98 μm (2), 53 μm (3), 34 μm (4), and in its unprotected form (2.5 wt % catalyst added to the resin; 5).

Catalyst stability was assessed by exposure to a resin mimic (with viscosity qualitatively similar to that of the Derakane 510A-40 resin) consisting of EPON 828 resin (un-reactive to free radicals), 14 wt % acetone, 1 wt % BPO and 0.1 wt % DMA. After exposure to the resin mimic for 24 h, the microspheres were filtered, washed with acetone and dried. The dried microspheres were then dissolved in cyclohexane and the ultraviolet-visible (UV-vis) absorption of the resulting solution was measured. Grubbs' first generation catalyst exhibits a characteristic visible absorption which has been attributed to metal to ligand charge transfer (MLCT).[13,14] In cyclohexane, this absorption occurs at λ_{max} = 527 nm with a molar absorptivity α = 467 M^{-1} cm^{-1}. Reaction of free radicals with the ruthenium catalyst complex changes the characteristics of this MLCT effect, decreasing the intensity of the visible absorbance band. Decrease in intensity of this diagnostic MLCT absorbance indicates a decrease in the concentration of active catalyst species.

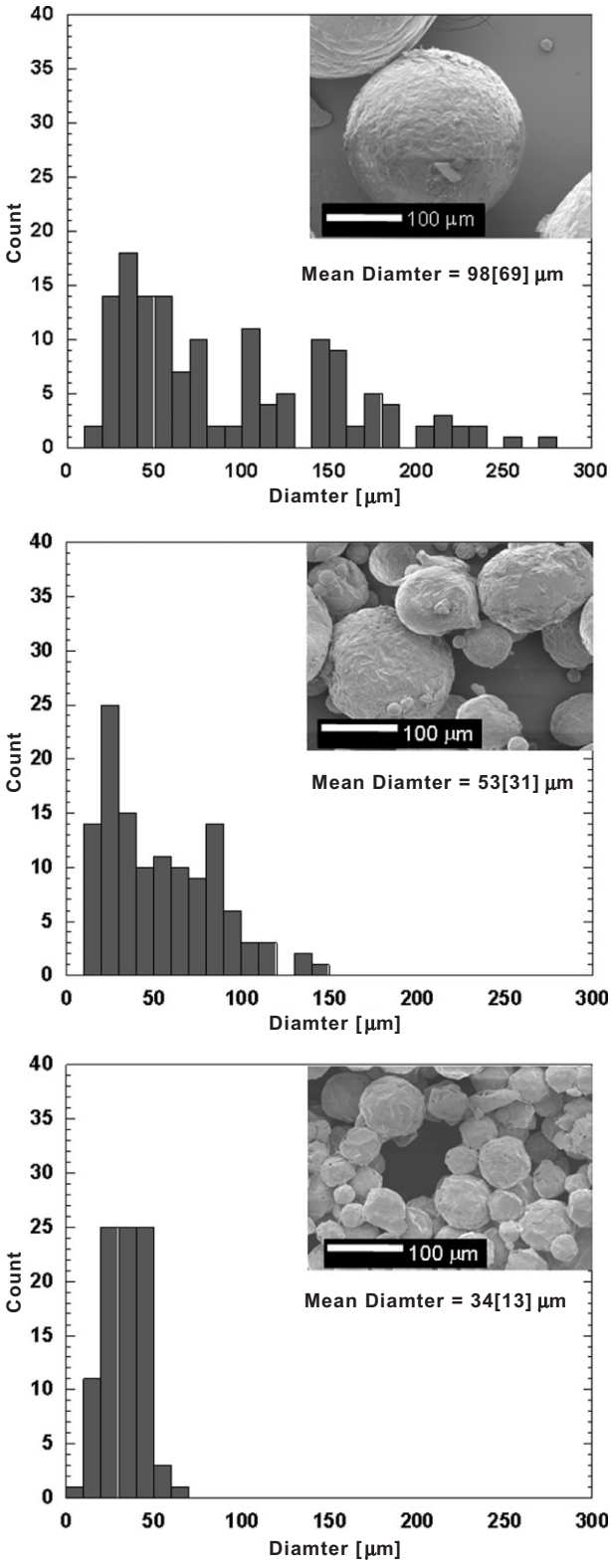

Figure 4. Comparison of ESEM images and size distributions of wax microspheres of three different sizes: a) 98[69] μm, b) 53[31] μm, and c) 34[13] μm (standard deviations in square brackets). Wax microspheres were synthesized by a hydrophobic congealable disperse phase encapsulation procedure. The 34 μm microspheres were obtained by modifying the viscosity of the wax using benzene, allowing smaller microspheres to be produced at similar shear rates as those used for larger microspheres.

ADVANCED FUNCTIONAL MATERIALS

Compared to the first control sample (Fig. 5, 1) which was exposed to the resin mimic alone, the 98 μm and 53 μm wax microspheres exhibited less than a 10 % decrease in absorbance after exposure to the same resin mimic containing BPO and DMA for 24 h (Fig. 5, 3 and 4). The 34 μm wax microspheres, which were prepared by a slightly modified procedure (see experimental section) showed slightly less protection (roughly 20 % decrease in absorbance; Fig. 5, 5) after exposure to the resin mimic containing BPO and DMA, relative to a control sample consisting of 34 μm wax microspheres (Fig. 5, 2) which were previously exposed to the resin mimic alone. The control sample prepared using the 34 μm microspheres and exposed to the resin mimic alone showed a decrease in absorbance compared to the control sample containing 98 μm microspheres. This decrease in absorbance observed is attributed to some decomposition during microsphere synthesis, presumably due to the elevated temperature involved in this procedure and the catalyst's thermal instability in solution.[15]

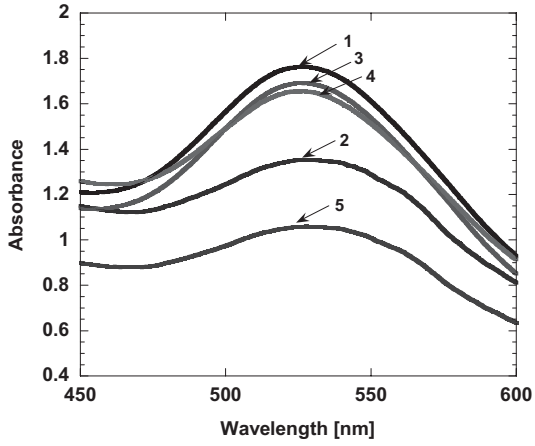

Figure 5. Representative UV-vis absorption curves measured in cyclohexane showing an evaluation of the degree of protection of the catalyst afforded by encapsulation in wax microspheres. Two control samples (1 and 2) were prepared for comparison since two different methods were used to synthesize the three different microspheres. The first control experiment (1) is for microspheres synthesized by the procedure reported by Rule and co-workers [5] (98 μm and 53 μm) exposed to the resin mimic alone. The second control experiment (2) is the exposure of microspheres prepared by pre-dissolving the catalyst in benzene (34 μm; see experimental section), to the resin mimic alone. The remaining experiments (3–5) depicted here are for samples containing catalyst protected in wax microspheres of sizes 98 μm (3), 53 μm (4), 34 μm (5) that were exposed to the resin mimic also containing BPO and DMA.

The activity of the catalyst embedded in the three different wax microspheres was quantified by monitoring the ROMP kinetics of *endo*-DCPD in the presence of these microspheres by *in situ* ^{1}H NMR spectroscopy. The rate constant measured for a control sample containing 98 μm catalyst microspheres previously exposed to the resin mimic excluding BPO and DMA was 3.0×10^{-4} s^{-1}. The rate constants measured for the 98 μm and 53 μm catalyst microspheres after exposure to the resin mimic containing BPO and DMA for 24 h were 2.9×10^{-4} s^{-1} and 2.7×10^{-4} s^{-1}, respectively. The rate constant measured for a second control sample containing 34 μm catalyst microspheres and previously exposed to resin mimic alone was 2.4×10^{-4} s^{-1}. The 20 % drop in catalyst activity between the two controls is due to the difference in the methods used to synthesize the microspheres and is consistent with the decrease in absorbance observed in the UV-vis experiment (Fig. 5). Finally, the rate constant measured for the sample containing the 34 μm catalyst microspheres after exposure to the resin mimic containing BPO and DMA for 24 h was 2.1×10^{-4} s^{-1}. Compared to their specific controls, the 98 μm, 53 μm, and 34 μm microspheres preserved 97 %, 90 %, and 88 % of catalyst activity respectively after exposure to the resin mimic containing BPO and DMA.

Encapsulation of the catalyst in wax also allowed Grubbs' catalyst to be incorporated into the matrix without significantly decreasing the degree of resin curing. However, as the microspheres became smaller, a decreasing initial rate and degree of cure of the resin was observed (Fig. 3). Presumably, as the surface to volume ratio increases, free radicals diffuse through the wax barrier and react with the catalyst.

Previously reported examples of ROMP-based self-healing materials[1–8] employed *endo*-DCPD as a healing agent. However, the *exo* isomer of DCPD exhibits an initial ROMP rate that is about 20 times that of the *endo* isomer.[16] The use of *exo*-DCPD as a healing agent for improved self-healing kinetics was explored in this study. Reference fracture tests[4] were used to evaluate *exo*-DCPD as a healing agent.

Epoxy vinyl ester fracture specimens with a tapered double cantilever beam (TDCB) geometry[4] were manufactured initially with no self-healing components. These samples were pin loaded to failure, after which the two halves were brought back in contact and healing agent (*exo* or *endo*-DCPD) pre-mixed with catalyst was manually injected into the crack. The specimens were then retested to failure after 24 h of healing at room temperature. Samples healed with *endo*-DCPD exhibited significantly lower average peak fracture load compared to *exo*-DCPD at 3×10^{-3} g mL^{-1} catalyst concentration (Table 1).

Table 1. Summary of reference test results comparing average healing efficiencies for epoxy vinyl ester samples. One standard deviation in square brackets.

Healing agent	Monomer:catalyst ratio	No. of samples	Average virgin peak load, P_c [N]	Average healed peak load, P_c [N]	Average healing efficiency, η [%]
endo-DCPD	300:1	4	71.50 [16.52]	15.43 [9.07]	22
endo-DCPD	40:1	4	72.14 [1.78]	33.43 [2.40]	46
exo-DCPD	300:1	5	70.55 [3.43]	34.63 [6.14]	49

To achieve the same level of healing (peak fracture load) roughly 8 times the catalyst concentration was required for healing with *endo*-DCPD. Since the amount of catalyst available in the crack plane is difficult to control, these results suggest that *exo*-DCPD will polymerize to a greater extent at lower catalyst concentrations and could potentially heal to a greater degree. Therefore *exo*-DCPD was used in subsequent studies as the healing agent for the epoxy vinyl ester self-healing system.

Self-activated fracture tests[4] were used to refine and optimize the healing performance of epoxy vinyl ester. In self-activated tests, only the catalyst phase is embedded within the matrix and the healing agent is delivered manually. Grubbs' catalyst was incorporated in the form of 98 μm wax microspheres, with each microsphere containing approximately 10 wt % catalyst. TDCB samples were loaded to failure, the two halves were then brought together, and a specified amount of *exo*-DCPD monomer was carefully injected into the crack. The amount of monomer delivered and the catalyst microsphere concentration were both observed to affect the recovery of mechanical properties as quantified by the peak fracture load and energy to failure of the healed sample (Fig. 6). Generally, healing performance appears to improve with both the amount of monomer delivered and catalyst microsphere concentration. The average peak fracture loads for the lower catalyst concentrations (5 wt % and 10 wt %, Fig. 6a) begin leveling off at a faster rate than the corresponding energy to failure data (Fig. 6b) possibly due to the increase in energy expected as further dissolution of catalyst microspheres results in increasingly plasticized poly(DCPD). Scanning electron microscope images of representative fracture surfaces reveal greater surface coverage (Fig. 7b and c relative to a) and increased thickness of the poly(DCPD) film with increased amount of DCPD injected into the crack. This observation is likely due to an increase in initial polymerization rates stemming from an increase in concentration of catalyst upon further dissolution of the catalyst microspheres.

Self-activated tests were also used to determine the effect of catalyst microsphere size on healing performance. During the healing event, smaller microspheres are expected to dissolve more rapidly, making catalyst availability on a specific fracture plane more uniform. Healing performance was therefore expected to increase with decreasing catalyst microsphere size to the extent that the catalyst in these microspheres is sufficiently protected from the harmful effects of the curing agents. Samples containing 53 μm microspheres exhibited the best healing performance as quantified by peak fracture loads (Fig. 8a) and energy to failure (Fig 8b). At the 34 μm microsphere size, healing performance drops presumably because of the decreased inherent catalytic activity of these microspheres as well as decreased protection from the curing agents (Fig 5). Furthermore, agglomeration of microspheres was problematic at the 34 μm size so that uniform dispersion was not achieved, leading to inefficient distribution of catalyst within the matrix and decreased healing performance.

Fully self-healing TDCB fracture evaluations were then undertaken in which catalyst microspheres were embedded in the epoxy vinyl ester matrix together with urea-formaldehyde microcapsules containing *exo*-DCPD healing agent. The catalyst concentration was varied between 10 and 15 wt % of 53 μm catalyst microspheres, since this size and concentration range produced the best healing performance in self-activated tests. Relatively large DCPD microcapsules ((250 ± 31) μm) were used in order to maximize delivery of monomer for best healing performance. Healing increased with microcapsule loading up to 15 wt %, after which diminishing gains in peak load (Fig. 9a) and energy to failure (Fig. 9b) were observed. A representative load-displacement curve for a sample containing 15 wt % catalyst microspheres and 15 wt % microcapsules

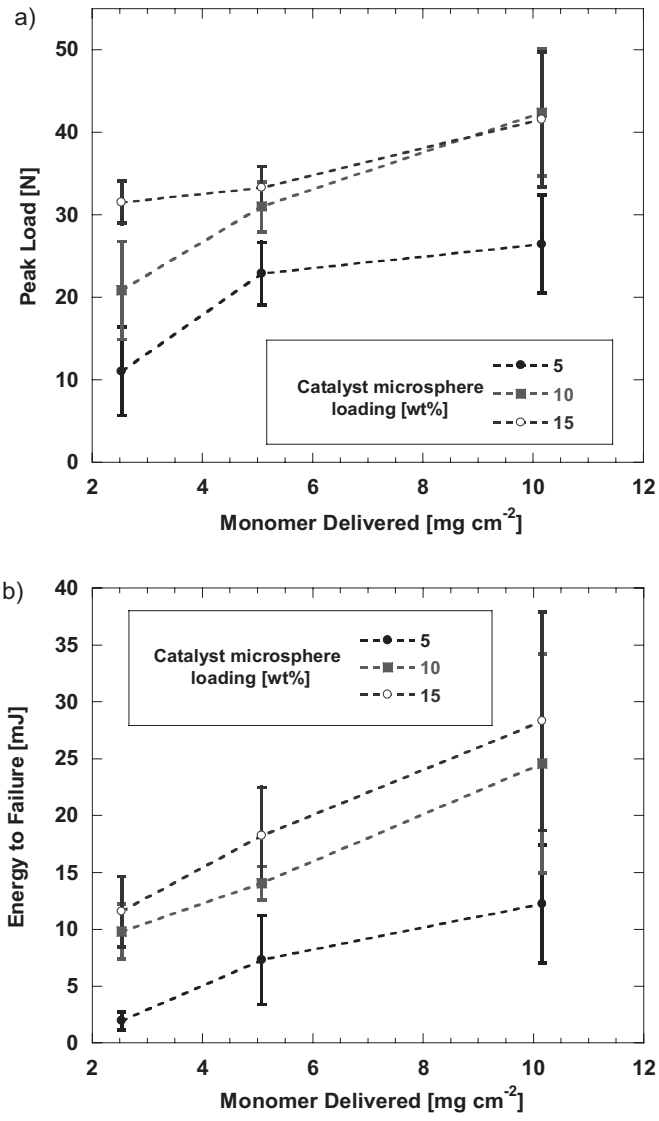

Figure 6. Fracture test results in terms of both a) peak load and b) strain energy to failure for self-activated samples healed with varying amounts of healing agent manually delivered to the crack plane. As indicated, three different catalyst microsphere concentrations (5 wt %, 10 wt % and 15 wt %) were used. Microsphere size was 98 μm for all tests. The error bars show the total range of results for 4–6 trials and the data points represent the average values.

ADVANCED FUNCTIONAL MATERIALS

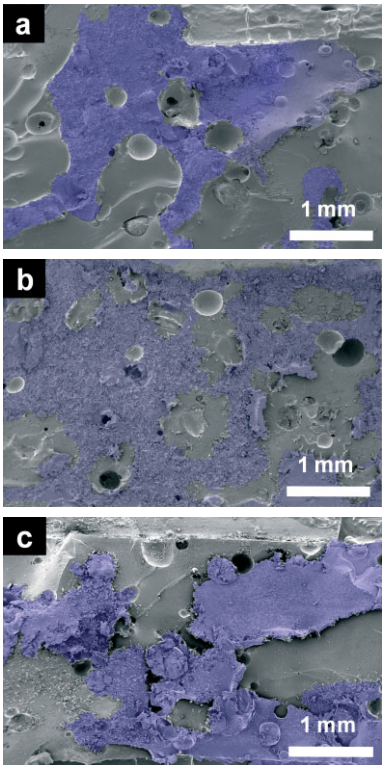

Figure 7. ESEM images of fracture surfaces showing partial poly(DCPD) coverage from a) 2.54 mg cm^{-2} DCPD, b) 5.08 mg cm^{-2} DCPD, and c) 10.16 mg cm^{-2} DCPD. In all three fracture planes shown here, concentration of catalyst microspheres was 10 wt % and catalyst microsphere size was 98 μm. Polymerized healing agent has been highlighted in blue.

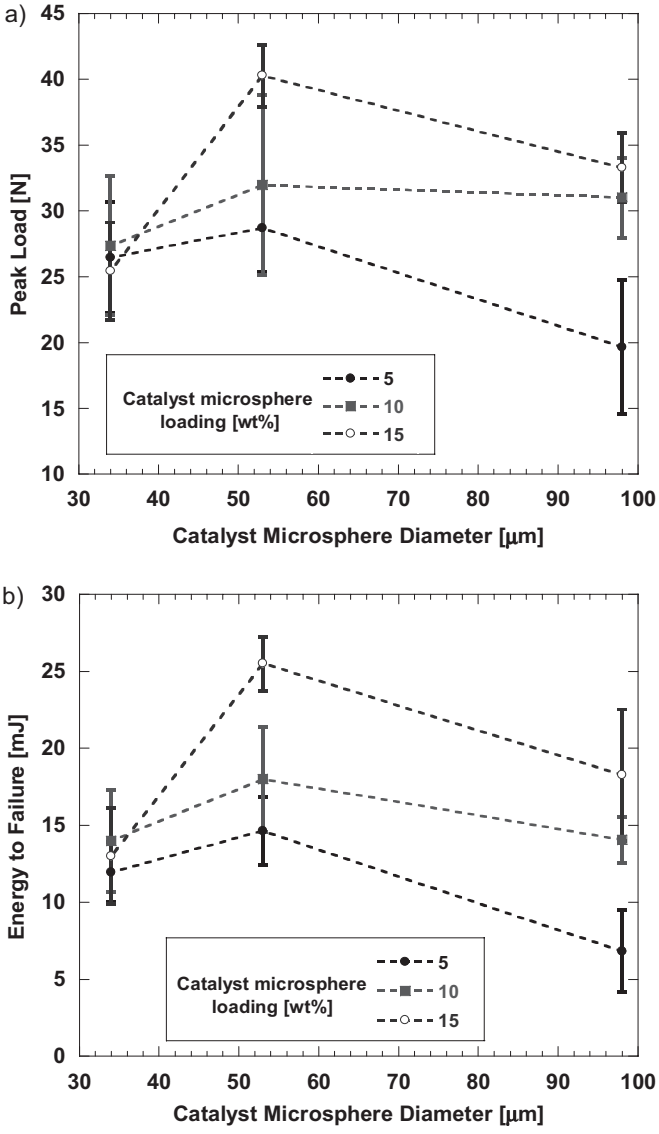

Figure 8. Fracture test results in terms of both a) peak load and b) strain energy to failure for self-activated samples containing catalyst microspheres of various diameters (98 μm, 53 μm, and 34 μm). As indicated, three different catalyst microsphere concentrations (5 wt %, 10 wt % and 15 wt %) were used. The error bars show the total range of results for 4–6 trials and the data points represent the average values.

shows a recovery of virgin mechanical properties of ca. 30 % for both the peak fracture load and energy to failure (Fig. 10a). It can be seen that the addition of self-healing components increases the virgin fracture toughness of the epoxy vinyl ester matrix, a result that appears to be quite general for self-healing polymers.[1,4–6,11] As such, comparison of the peak fracture load and energy to failure of this representative healed sample to the neat matrix resin (Table 1) yields a recovery of mechanical properties of 50 %. The corresponding fracture surface for this specimen after healing (Fig. 10b) shows ruptured microcapsules and the poly(DCPD) formed in the crack plane after self-healing has occurred.

In situ self-healing kinetics was determined by evaluating the self-healing performance of a series of 10 samples containing 15 wt % catalyst microspheres and 15 wt % DCPD microcapsules. After the initial virgin fracture, healing was allowed to proceed for a specified period of time ranging from 2.5 min to 48 h. Significant recovery of virgin mechanical properties was observed within 2.5 min (Fig. 11), consistent with previously reported observations that gelation of *exo*-DCPD occurs in less than 1 min in the presence of 0.2 wt % Grubbs' catalyst.[16] A change in the slope of the healing kinetics curve is observed at 6 h; however, the healing efficiency continues to improve up to 48 h.

3. Conclusions

We have successfully demonstrated a materials system capable of autonomic healing of commercially significant epoxy vinyl esters at room temperature via ROMP. Protection of Grubbs' catalyst is crucial in preserving ROMP catalytic activity, and avoiding deleterious effects on the matrix. Wax microspheres with a mean diameter of 53 μm provided adequate protection of the catalyst phase while enabling good self-healing efficiency. Self-healing performance improved with increased catalyst microsphere and DCPD microcapsule concentrations up to 15 wt %.

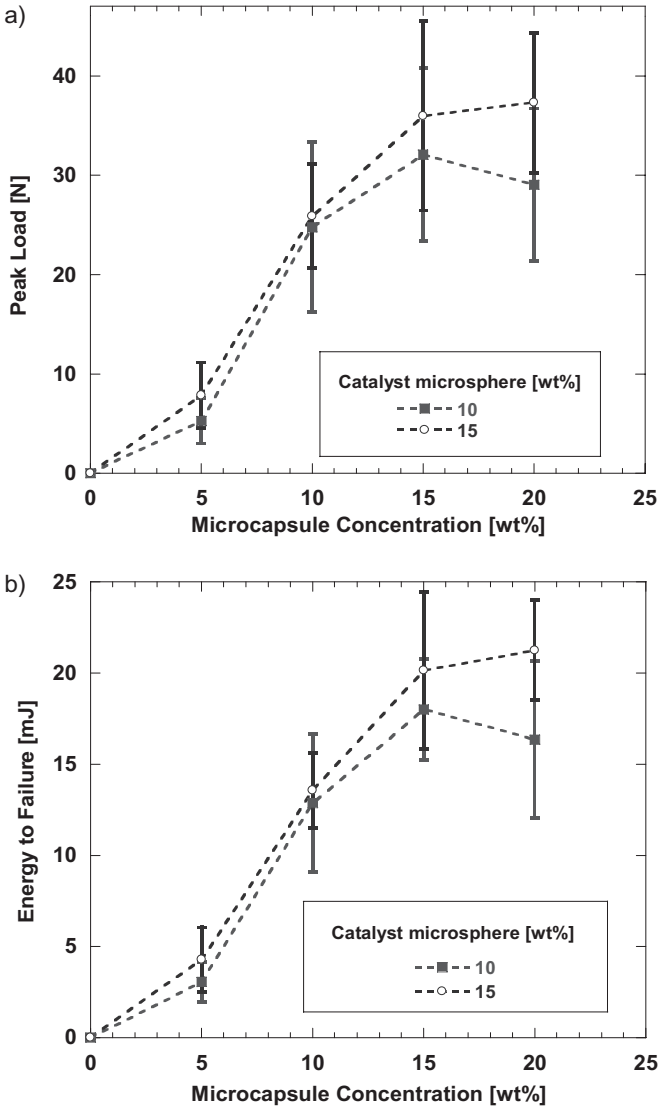

Figure 9. Fracture test results in terms of both a) peak load and b) strain energy to failure for *in situ* samples containing varying DCPD microcapsule loadings. As indicated, catalyst microsphere (53 μm) concentrations were 10 wt % and 15 wt %. In the absence of microcapsules, peak fracture load and energy to failure are zero for both 10 wt % and 15 wt % catalyst microsphere concentrations. The error bars show the total range of results for 4–6 trials and the data points represent the average values.

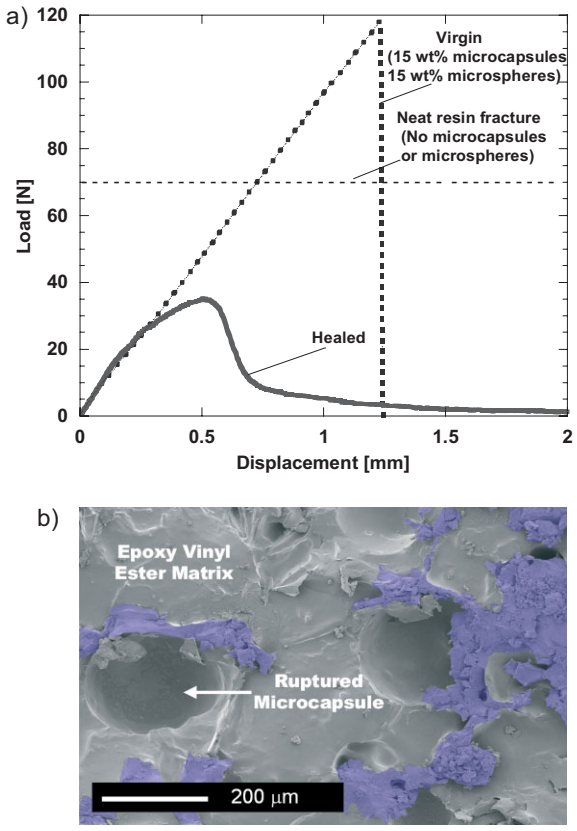

Figure 10. a) Representative load-displacement curve for a sample containing 15 wt % catalyst microspheres and 15 wt % microcapsules. Average peak load for virgin reference samples is included for comparison. b) ESEM image of corresponding fracture surface. poly(DCPD) plasticized with wax is observed around the ruptured microcapsules and is highlighted in blue.

Self-healing in the materials system reported here was successfully achieved using smaller catalyst microspheres than has been previously reported.[5] For fiber-reinforced composites, the use of smaller self-healing components is critically important to maintain high structural efficiency and for seamless integration into the laminate architecture. The use of *exo*-DCPD as a healing agent significantly improved the self-healing kinetics compared to previously reported ROMP-based self-healing polymers[4] and recovery of mechanical properties was observed within 2.5 min. This improvement in healing kinetics could translate into improved fatigue performance and shorter rest periods in the loading cycle than have been previously demonstrated in self-healing systems employing *endo*-DCPD as the healing agent.[8]

4. Experimental

Derakane 510A-40 epoxy vinyl ester was obtained from Ashland Chemical Company and the curing agents, benzoyl peroxide (BPO) and dimethylaniline (DMA) were purchased from Sigma-Aldrich. Bis(-tricyclohexylphosphine)benzylidene ruthenium (IV) dichloride (first generation Grubbs' catalyst) was obtained from Sigma–Aldrich and recrystallized by freeze-drying as reported elsewhere [17]. *endo*-DCPD was purchased from Acros Organics and *exo*-DCPD was synthesized as reported elsewhere [18]. Both isomers were distilled and stabilized with 150 ppm of *tert*-butylcatechol before use. *exo*-DCPD used in this study was determined by gas chromatography to contain 13 % *endo*-DCPD. The viscosity of *exo*-DCPD was modified to match that of *endo*-DCPD by addition of 1 wt % polystyrene (M_N = 53000; PDI = 4.79, Aldrich). Microcapsules containing *exo*-DCPD were synthesized using the previously described procedure [19]. An average microcapsule diameter of (250 ± 31) μm was obtained at 350 rpm stirring rate.

The effect of the curing agents BPO and DMA on Grubbs' catalyst was evaluated by *in situ* NMR spectroscopy on a Varian UNITY INOVA 500 NB instrument. Three experiments were performed to determine the effects of BPO (1 wt %) and DMA (0.1 wt %) first separately, and then together at the standard concentrations used for

ADVANCED FUNCTIONAL MATERIALS

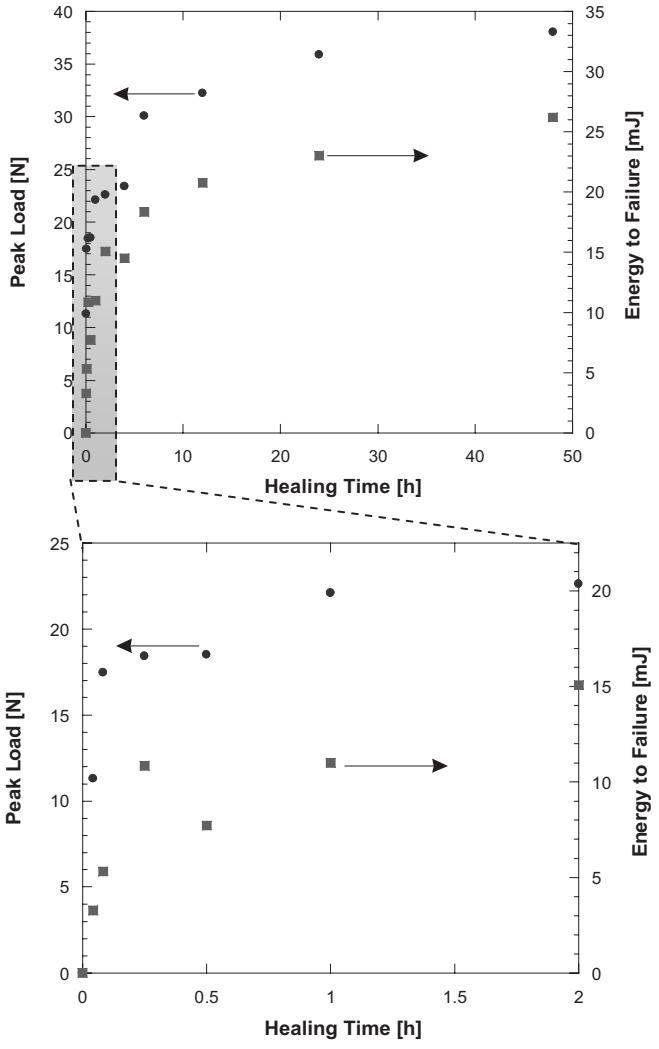

Figure 11. Self-healing performance of *in situ* samples containing 15 wt % catalyst microspheres and 15 wt % microcapsules as a function of healing time.

curing the epoxy vinyl ester. Three NMR tubes each containing a solution of Grubbs' catalyst in benzene-d_6 and separate vials containing solutions of BPO or DMA also in benzene-d_6 were prepared in an argon-filled glove box. The tubes and vials were then capped with septa and sealed with parafilm and electrical tape successively. For each experiment, the instrument and the inserted tube (containing catalyst solution) were brought to 25 °C. The tube was then ejected and BPO and/or DMA stock solutions were added, followed by mesitylene (internal standard, 10 μL). Each tube re-inserted into the instrument contained Grubbs catalyst (0.012 M) in a total of 0.8 mL of benzene-d_6 and either BPO (1 wt %, 0.041 M), DMA (0.1 wt %, 0.0083 M) or both. Spectra were taken at regular intervals until the completion of the experiment.

Various sizes of catalyst microspheres were synthesized for use in this study. A previously reported congealable disperse phase encapsulated procedure [5] was used to synthesize 98 μm and 53 μm microspheres by using stirring rates of 1000 and 2500 rpm, respectively. Poly(vinyl alcohol) (PVA, 87–89 % hydrolyzed, M_N = 85000–124000, 0.25 wt %) was used as a surfactant in the aqueous solution in the place of poly(ethylene-*co*-maleic anhydride). Smaller microspheres were synthesized by a slight modification to this procedure. The catalyst (0.5 g) was dissolved in dry benzene (5 g) in an argon-filled glove box. Paraffin wax (5 g) was then added and the vial was sealed and removed from the glove box. The vial was then submerged in the same 80 °C water bath that contained the stirring aqueous solution. After about 5 min, the wax formed a homogenous liquid phase with the benzene in which the catalyst was completely dissolved. The contents of the vial were then poured into the aqueous solution which was being stirred at 2500 rpm. After 2 min, ice water (400 mL, 0 °C) was quickly added to the aqueous solution and the stirring stopped. The microspheres were collected by filtration and dried under vacuum for 24 h. The size distributions and environmental scanning electron microscopy (ESEM) images of the microspheres are compared in Figure 4. All microspheres were synthesized using 10 wt % catalyst in wax.

The degree of catalyst protection afforded by encapsulation in wax was evaluated in an epoxy resin (EPON 828, Miller Stephenson) diluted with 14 wt % acetone to qualitatively match the viscosity of the epoxy vinyl ester resin. Wax microspheres (300 mg) of the three different sizes (34 μm, 53 μm, and 98 μm) were weighed into separate 20 mL vials. The diluted epoxy resin (3 g) containing 1 wt % BPO and 0.1 wt % DMA was added to each vial. The vials were capped and the contents were stirred for 24 h. The contents of each vial were then filtered, washed with acetone and dried under vacuum. In the control experiments, wax microspheres containing catalyst (34 μm, 53 μm, and 98 μm) were stirred in the diluted epoxy resin without BPO or DMA and stored for 24 h. The resulting catalyst microspheres from all the tests described above were washed with acetone and dried under vacuum. In all cases, the resulting catalyst microspheres were then dissolved in cyclohexane to make (30 ± 0.6) mg mL^{-1} solutions. The ultraviolet-visible absorbances of these solutions were measured on a Shimadzu UV-2410PC spectrophotometer. *In Situ* ^{1}H NMR kinetic measurements of the ROMP of DCPD in the presence of catalyst microspheres after exposure to resin mimic alone (control samples) and resin mimic containing BPO and DMA were performed as described elsewhere [5]. Each sample contained 70 mg of wax microspheres containing 10 wt % Grubbs' catalyst (0.0085 mmol).

The effect of catalyst and degree of catalyst protection on the curing kinetics of the epoxy vinyl ester resin was evaluated by Differential Scanning Calorimetry (DSC) experiments performed on a Mettler Toledo DSC821^e. Dynamic DSC experiments were performed on a resin sample containing 1 wt % BPO and 0.1 wt % DMA by heating the sample from 25 °C to 250 °C at 10 °C min^{-1} to determine the total heat of reaction ((217.9 (11.5) J g^{-1}, determined from 4 trials). A series of isothermal curing experiments (25 °C, 120 min) was also performed in which each sample contained 1 wt % BPO and 0.1 wt % DMA and either 1–2.5 wt % of unprotected Grubbs' catalyst or 10 wt % of catalyst microspheres containing 10 wt % Grubbs catalyst of various sizes (overall catalyst loading was 1 wt %). A control isothermal experiment in which no catalyst was added was also performed. The DSC cell was swept by a constant flow of N_2 at 80 mL min^{-1} in all experiments. Degree of cure (α_t) was determined as a function of time using the following equation:

$$a_t = 100\frac{Q_t}{Q_T} \tag{1}$$

where Q_t is the reaction heat at time t, and Q_T is the total heat of polymerization [20,21].

Fracture specimens were prepared with a tapered double cantilever beam (TDCB) geometry using Derakane 510A-40 epoxy vinyl ester resin cured with 1 wt % BPO and 0.1 wt % DMA. The specimens were cured for 24 h at room temperature before performing fracture tests. Self-healing components (microcapsules containing DCPD and catalyst microspheres) were stirred directly into the resin prior to pouring into the TDCB molds.

Fracture tests followed established procedure [4] in which a razor blade was used to initiate a pre-crack. The specimens were then pin loaded and tested under displacement control at a rate of 5 μm s^{-1}. Once completely fractured, the two halves of each specimen were brought back in contact and left to heal for 24 h (unless otherwise noted) at room temperature before retesting to failure. Self healing

performance was quantified by the peak load achieved during fracture and by the strain energy to failure for each healed specimen as given by the area under the load-displacement curve [5]. An average healing efficiency (η_{avg}) can be defined based on average peak fracture loads (P_c) as

$$\eta_{avg} = \frac{Avg[P_c^{Healed}]}{Avg[P_c^{Virgin}]} \quad (2)$$

or in terms of average energy to failure (U_c) as

$$\eta_{avg}^{U_c} = \frac{Avg[U_c^{Healed}]}{Avg[U_c^{Virgin}]} \quad (3)$$

In all plots (except representative load-displacement plots), each point represents the average of between 4 and 6 trials, and the error bars are +/– one standard deviation.

Received: April 12, 2007
Revised: June 28, 2007
Published online: December 18, 2007

[1] S. R. White, N. R. Sottos, P. R. Guebelle, J. S. Moore, M. R. Kessler, S. R. Sriram, E. N. Brown, S. Viswanathan, *Nature* **2001**, *409*, 794.
[2] M. R. Kessler, S. R. White, *Composites Part A* **2001**, *32*, 683.
[3] M. R. Kessler, N. R. Sottos, S. R. White, *Composites Part A* **2003**, *34*, 743.
[4] E. N. Brown, N. R. Sottos, S. R. White, *Exp. Mech.* **2002**, *42*, 372.
[5] J. D. Rule, N. R. Sottos, S. R. White, J. S. Moore, *Adv. Mater.* **2005**, *17*, 205.
[6] E. N. Brown, S. R. White, N. R. Sottos, *J. Mater. Sci.* **2004**, *39*, 1703.
[7] E. N. Brown, S. R. White, N. R. Sottos, *Compos. Sci. Technol.* **2005**, *65*, 2466.
[8] E. N. Brown, S. R. White, N. R. Sottos, *Compos. Sci. Technol.* **2005**, *65*, 2474.
[9] J. W. C. Pang, I. P. Bond, *Compos. Sci. Technol.* **2005**, *65*, 1791.
[10] J. Y. Lee, G. A. Buxton, A. C. Balazs, *J. Chem. Phys.* **2004**, *121*, 5531.
[11] C. W. Biewlawski, R. H. Grubbs, *Prog. Polym. Sci.* **2007**, *32*, 1.
[12] S. Cho, H. M. Andersson, S. R. White, N. R. Sottos, P. V. Braun, *Adv. Mater.* **2006**, *18*, 997.
[13] M. S. Sanford, J. A. Love, R. H. Grubbs, *J. Am. Chem. Soc.* **2001**, *123*, 6543.
[14] S. M. Hansen, F. Rominger, M. Metz, P. Hofmann, *Chem. Eur. J.* **1999**, *5*, 557.
[15] *Handbook of Metathesis* (Ed: R. H. Grubbs), Wiley-VCH, Weinheim **2003**.
[16] J. D. Rule, J. S. Moore, *Macromolecules* **2002**, *35*, 7878.
[17] A. S. Jones, J. D. Rule, J. S. Moore, S. R. White, N. R. Sottos, *Chem. Mater.* **2006**, *18*, 1312.
[18] G. L. Nelson, C.-L. Kuo, *Synthesis* **1975**, 105.
[19] E. N. Brown, M. R. Kessler, N. R. Sottos, S. R. White, *J. Microencapsulation* **2003**, *20*, 719.
[20] M. R. Kessler, S. R. White, *J. Polym. Sci. Part A* **2002**, *40*, 2373.
[21] C. Elvira, B. Levenfeld, B. Vázquez, J. San Román, *J. Polym. Sci. Part A* **1996**, *34*, 2783.